Werk

Jahr: 1979
Kollektion: fid.geo
Signatur: 8 Z NAT 2148:46
Digitalisiert: Niedersächsische Staats- und Universitätsbibliothek Göttingen
Werk Id: PPN1015067948_0046
PURL: http://resolver.sub.uni-goettingen.de/purl?PPN1015067948_0046

LOG Id: LOG_0010
LOG Titel: Ionospheric absorption and profiles of electron density and loss-rate in the lower ionosphere
LOG Typ: article

Übergeordnetes Werk

Werk Id: PPN1015067948
PURL: http://resolver.sub.uni-goettingen.de/purl?PPN1015067948
OPAC: http://opac.sub.uni-goettingen.de/DB=1/PPN?PPN=1015067948

Contact

Niedersächsische Staats- und Universitätsbibliothek Göttingen
Georg-August-Universität Göttingen
Platz der Göttinger Sieben 1
37073 Göttingen
Germany
Email: gdz@sub.uni-goettingen.de

J. Geophys. 46, 23–33, 1979

Journal of Geophysics

Ionospheric Absorption and Profiles of Electron Density and Loss-Rate in the Lower Ionosphere*

K.M. Kotadia and A. Gupta

Physics Department, Gujarat University, Ahmedabad 380009, India

Abstract. A1-absorption measurements on 1.8, 2.2 and 2.5 MHz frequencies are being made at Gujarat University, Ahmedabad (23°N, 72.6°E; mag. dip 34°N) since April, 1972. Partial reflection measurements were started in 1974 by *Physical Research Laboratory* (PRL) and the Ionosonde has been in operation since 1952 just nearby. The rocket experiment facilities were established in India at the equatorial station Thumba in 1963. In this paper, we have combined the results of all the above ground-based and rocket-borne experiments to determine the electron density and effective loss-rate profiles in the height range 65–110 km for quiet-sun low solar activity period. Cira (1972) Atmospheric model is used for concentrations of various gases, pressure and temperature. Profiles of nitric oxide and metastable molecular oxygen used in our computations are those due to Meira (1971) and Huffman et al. (1971).

It is shown that the *N-h* profile so obtained indicates a stratification intermediate between the *D*-layer maximum and the *E*-layer, and this is clearer at smaller *solar zenith angle* (SZA) times. This stratification seems to have a maximum electron density around 10^4 electrons/cm^3 at a height of about 95 km. The effective loss-rate is found to be greater at heights below 80 km and smaller at heights above 90 km than the dissociative recombination coefficient to the extent of an order of magnitude depending on the time of the day. The results are discussed in context to the negative ions, heavy metallic ions and the gas composition.

Key words: Ionospheric absorption – Electron density – Loss rate – Lower ionosphere.

1. Introduction

The ionospheric absorption of a radio wave at a given frequency is a function of the refractive index, electron density and the collision frequency in the medium

* Dedicated to Professor Dr. K. Rawer on the occasion of his 65th birthday

0340-062X/79/0046/0023/02.20

through which the wave travels. The refractive index at a particular height is itself determined by the electron density N, electron collision frequency and the effective frequency ($f \pm f_H$). The collision frequency depends on the neutral particle concentration, electron and ion densities and electron temperature. The collision frequency that is important in the lower ionosphere is that of electrons with neutral molecules.

Here, the ionospheric absorption data are used to fill the gap suitably in the electron density profile obtained by other methods such as rocket, partial reflections, and the ionosonde measurements. At Ahmedabad, we have at the Gujarat University an INDO-GDR collaboration A1-absorption project in operation since 1972. We have also a joint cooperative project with Physical Research Laboratory (PRL) on partial reflections since 1974 and the ionosonde is being run by the P.R.L. since 1952. Quite a large number of rocket flights carrying different kinds of payloads have been made since the establishment in 1963 of the rocket launching centre at the equatorial station, namely Thumba (8°33′N, 76°56′E; $I = 0.8°$S) but these were scattered instances as regards days, solar zenith angle and solar activity.

For estimation of effective loss-rate, we need to know the total electron-ion pair production rate which requires the knowledge of concentrations of various gas species and the fluxes of various ionizing radiations. In particular, here we have produced average results for the quiet-sun conditions during minimum solar activity ($F_{10.7} < 80$ U; 1 U $= 10^{-22}$ W m^{-2} Hz^{-1}) at solar zenith angle (SZA) 30°–65° in the months of January, February, and March, 1975.

2. Atmospheric Model

The first atmospheric model giving pressure, density, mean molecular mass, temperature etc. was proposed in 1962 (U.S. standard Atmosphere 1962). Since then, many new observations have been made using ground-based, balloon and spacecraft techniques and improved computer modelling methods. The latest model used in our computations is the Cira, 1972 atmospheric model which is essentially based on the works of Groves (1971) and Jacchia (1971). In the calculation of ion-production rate from 60 km to 110 km altitudes, we have to consider the atmospheric model at height upto 160 km since the principal ionizing radiations responsible in the lower ionosphere begin to be attenuated on penetrating to heights from the level of 160 km downwards. The major constituents of the gas being ionized are N_2, O_2, and O and the minor constituents are the nitric oxide, NO, and the metastable oxygen, $O_2(1\Delta g)$. The latter two, though minor, are the main gases contributing to the middle D-region ionization. The models for N_2, O_2, and O are adopted from the Cira (1972), that of NO is due to Meira (1971) and the one for $O_2(1\Delta g)$ is due to Huffman et al. (1971). The profile of [NO] is believed to be nearly the same at heights above 70 km at different SZA's. Meira's model is still considered reasonably good for calculation of ion-production rate.

3. Collision Frequency

Following relations are used to calculate the collision frequency at different heights

$$\nu_{en} = 6.5 \times 10^5 \, p \quad \mathrm{s}^{-1}$$

Piggott and Thrane (1966). According to Banks (1966),

$$\nu_{ei} = 3.6 \times \mathrm{N} \, \mathrm{Te}^{-1.5} \ln(2 \times 10^4 \, \mathrm{Te}^{1.5}/\mathrm{N}^{0.5})$$

and

$$\nu_{eo} = [0] \; (1.88 \times 10^{-10} \, \mathrm{Te}^{0.5}).$$

In the above relations, p is pressure in Pa (or nt.m^{-2}), N is electron density in m^{-3}, Te is electron temperature in °K and [0] atomic oxygen concentration in m^{-3}. ν_{ei} and ν_{eo} are relatively unimportant in the lower ionosphere. There is some diurnal variation in pressure ranging from 0.1 to 0.2 Pa at 95 km with maxima at about 1400 and 0200 h and minima at 0800 and 2000 h but it reduces to very small variation at 65 km. Also at low latitudes, there is a seasonal variation in pressure with a minimum value 0.075 Pa in January and maximum value 0.105 Pa in September at 95 km altitude, with another subsidiary maximum in April. These variations in pressure produce changes accordingly in the collision frequency. The contribution to absorption of radio waves due to ionization and collision frequency below 70 km is very small.

4. Ion-Production Rate

The photo-ionization rate of a molecular or atomic gas species due to the absorption of ionizing radiations entering into the atmosphere is calculated by using the formula

$$q(z, \chi) = \phi(\lambda_j, z, \chi) \sum_j \gamma_j(\lambda) \, \sigma_{aj}(\lambda) \, n_j(z)$$

where j denotes j^{th} constituent of the gas, σ_{aj}, γ_j and n_j are respectively the absorption cross-section, ionization efficiency and number density of the j^{th} gas constituent, λ_j is the largest wavelength of the radiation capable of ionizing that constituent. $\phi(\lambda_j, z, \chi)$ is the total radiation flux of wavelength λ_j at solar zenith angle χ that is available after penetration to the height z. This flux at wavelength λ is given by the expression

$$\phi_\lambda(z, \chi) = \phi_{o\lambda} \exp\left[-\sum_j \sigma_{aj} \int_z^\infty n_j(l) \, dl\right]$$

in which $\phi_{o\lambda}$ is the flux of radiation of wavelength λ at the top of the atmosphere. The integral in the bracket gives the total number of particles

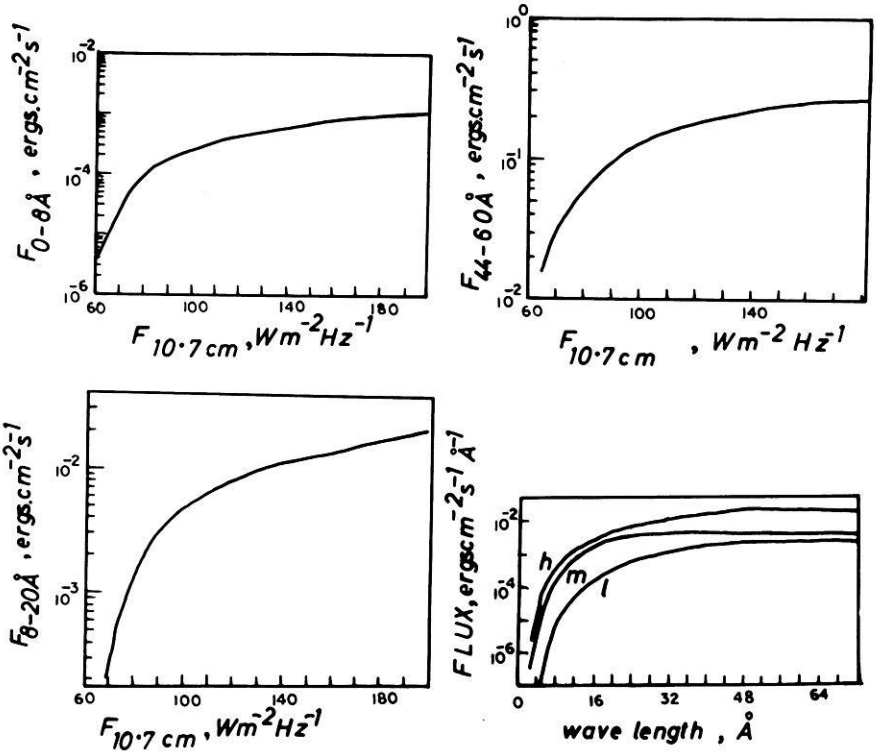

Fig. 1. Solar X-ray fluxes in 0–8 Å, 8–20 Å, and 44–60 Å bands against 10.7 cm solar radio flux, and X-ray spectrum for high, medium and low solar activity in the wavelength range 0 to 72 Å. $F_{10\cdot7}$ is in units of 10^{-22}

$S(z, x)$ of j^{th} gas constituent of spherically symmetric atmosphere in a unit column along the direction of the sun-rays from the level z of interest towards the sun (here upto 50 km radially above height z since the radiations concerned are absorbed in that region). This was calculated for different SZA values.

5. Ionizing Radiations and Cross-Sections

The total ion-production rate for all gases due to different radiations passing through them is obtained by summing up the q-rates for each gas produced by the radiations of wavelength ranging from 1 Å–1215·7 Å. The fluxes of these ionizing radiations, the absorption cross-sections and ionization-efficiency of a particular gas due to a particular radiation are now available in the richly published literature as well as Institutional Reports (Hinteregger et al., 1965; Hinteregger, 1970; Swider, 1969; Manson, 1972; Hall et al., 1965; Vidal-Madjar et al., 1973; Heroux and Higgins, 1977; Ivanov-Kholodnyi and Firsov, 1974; Horan, 1970; Loidl and Schwentek, 1977; Schmidtke, 1976). An average picture of the variation of flux in the X-ray spectrum with solar activity is shown in Fig. 1. The flux of the radiation at 1–3 Å remains below the measurable level for

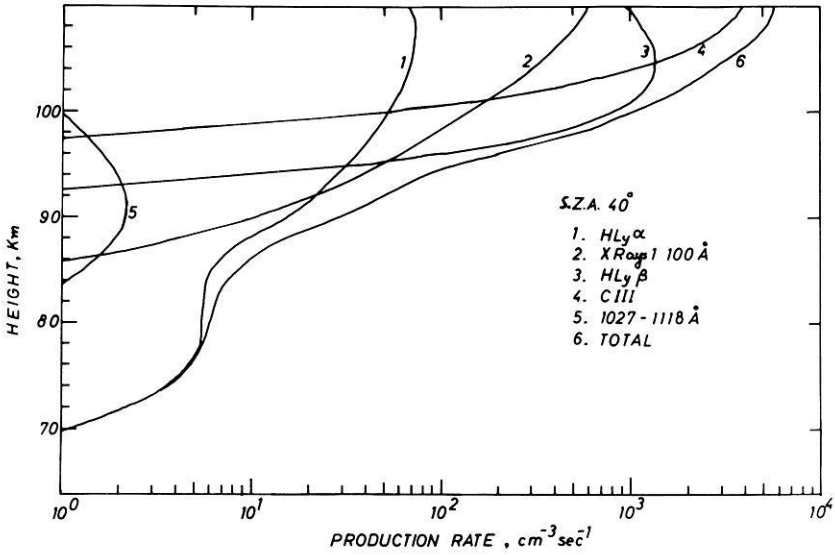

Fig. 2. Ion-production rate of various gas constituents in the height range 60–110 km due to different radiations for solar zenith angle 40°

most of the solar cycle period, and the ionization produced by such radiation at heights below 70 km does not contribute significantly to the radio wave absorption. A table of a few representative values of these fluxes was given in our earlier paper (Chhipa and Kotadia, 1978). The ion-production rates including the effects of background galactic cosmic rays and scattered geocoronal Lyman-alpha and Lyman-beta radiations were calculated for different solar zenith angles and here only one of them is shown in Fig. 2 for SZA 40°.

6. *N-h* Profiles

In-situ measurements of electron density have been made by various methods of rocket-probing. However, these have been under different conditions at different places. They seem to be so scattered in time and place that the material is insufficient for deducing a picture of general behaviour of the ionosphere, and particularly of the lower ionosphere where the situation is complicated by collisions, ion kinetics, uncertain loss processes and turbulent wind motions. However, the regular ground-based experiments such as ionosonde, absorption, partial reflections, wave-interaction, incoherent back-scatter and field-strength measurements at *vlf*, *lf*, *mf*, and *hf* can provide good amount of material to study the day-to-day variations and regular features of the ionosphere. As such, these experiments would continue to be powerful supporting tools in the investigations of the middle and the upper atmosphere. Here we have tried to combine the results obtained by ionosonde, A1-absorption and partial reflections for the height range 74–110 km, and rocket data at lower heights where

the ionospheric conditions are believed not to undergo significant changes with time and solar activity. *N-h* profiles available from several rocket flights in the height range 65–74 km are adjusted suitably for the low solar activity such that their average becomes continuous with the mean *N-h* profile obtained from partial reflections measurements. This brings the profile upto 88 km altitude. From the ionosonde *foE* and *hmE* data ($hmE = 105$ km around noontime), the *N-h* profile is drawn from *E*-layer maximum down to a height one-half the semithickness below the *hmE* level assuming parabolic distribution of electron density. *hmE* is supposed to vary according to the relation

$$hmE = 105 + H \ln(\sec \chi)$$

where the scale height H may change from 8 km at noon to 15 km near the sunrise and sunset times. The gap in the *N-h* profile in the height range 88 km to the lower half-thickness region of the *E*-layer has to be filled in such a way that the computed absorption and the virtual height of reflection at three radio frequencies agree reasonably with the observed values of absorption and virtual height. This will lead to the profile construction upto the height at which the electron density corresponds to the highest frequency, 2.5 MHz, used in our A1-absorption measurements.

In the computation of absorption coefficient, use is made of the Sen-Wyller generalised magnetoionic theory without recourse to QL or QT approximation. The computer program also takes care of converting the true height into virtual height. The lower part of the ionosphere under question is divided into slabs of thickness 1 km and absorption in each such slab is found. The slab-thickness is reduced as we go higher up, finally taking slabs of thickness 10 m near the level of reflection. The total absorption is then found by adding up absorption calculated for all such slabs and then multiplying the sum by 2 for up and down journey of the wave. The lowest frequency in our case is 1.8 MHz. Assuming on the basis of intuitive thinking, a kind of exponential profile passing through the point of reflection at 1.8 MHz and the points at ± 1.5 km, the upper point having greater electron density then at the lower point, absorption *Ldb* and h' are computed and compared with the observed values. If they do not agree, the points above and below the level of reflection are shifted upwards or downwards in height or laterally to lower or higher values of N (which amounts to changing the exponential shape of the profile) so that ultimately after a number of calculations and recalculations, the calculated and measured L_{db} and h' at the stated frequency agree well within experimental error. The process is then repeated in a similar way for the other two frequencies 2.2 and 2.5 MHz. The profile finally arrived at up to the reflection level at 2.5 MHz is then smoothly joined up with the *E*-layer profile obtained from the ionosonde data. Figure 3 gives the average *N-h* profiles thus completed for the month of March, 1975 at SZA 30°, 42°, and 65° C. It may be seen that the thus-found *N-h* profiles show the *D*-layer maximum electron density around 10^3 to 2×10^3 electrons/cm^3 at 82 to 85 km depending on the solar zenith angle. They also indicate another maximum at about 95 km with N around 10^4 electrons/cm^3. The cusp of such a maximum is clearer at lower solar zenith angles, but it is almost absent at high

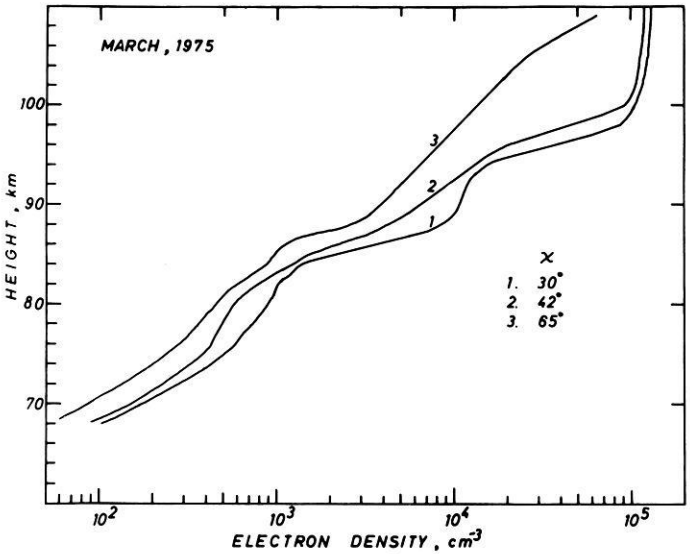

Fig. 3. Electron density distribution with height at SZA 30°, 42°, and 65° in March, 1975 under quiet-sun low solar activity conditions

values of SZA in winter months. Figures 4 and 5 give the N-h profiles for January and February, 1975 and the features of the stratification intermediate between the D-layer maximum and the bottom of the E-layer as described above are amply clear in these profiles also. Such intermediate stratifications were also reported by Bremer and Singer (1977) from their studies on A3 *lf* and *mf* absorption measurements. Mechtly and Bowhill (1972) had earlier noticed mild inflection at around 95 km in their rocket-measured N-h profiles during quiet-sun periods.

7. Effective Loss-Rate of Ionization

Having got the N-h and Q-h profiles, we now proceed to determine the $\alpha_{\text{eff}}-h$ profiles using the relation $\alpha_{\text{eff}}=Q/N^2$ where α_{eff} is the effective loss-rate or recombination coefficient. In the lower ionosphere, this is more accurately expressed as $\alpha_{\text{eff}}=(1+\lambda)\ (\alpha_d+\lambda\alpha_i)$ where $\lambda=N^-/N$, α_d is dissociative recombination coefficient, α_i is ion-ion neutralization rate and N^- is negative ion concentration. The ratio Q/N^2 is calculated for different heights and the results are shown in Fig. 6. It also gives mean α_{eff} for SZA 30°–50°. The effective α_d, i.e., total of electron recombination rates with all the molecular positive ions is based on theoretical models (not shown in the figure) rapidly increases at heights below 90 km and attains a constant value below 80 km as well as in the 90–95 km height region (Taubenheim et al., 1975). The transition region within the 80–90 km region may move up with increase in solar zenith angle. It is interesting to note that α_{eff} also shows a transition region similar to that for α_d.

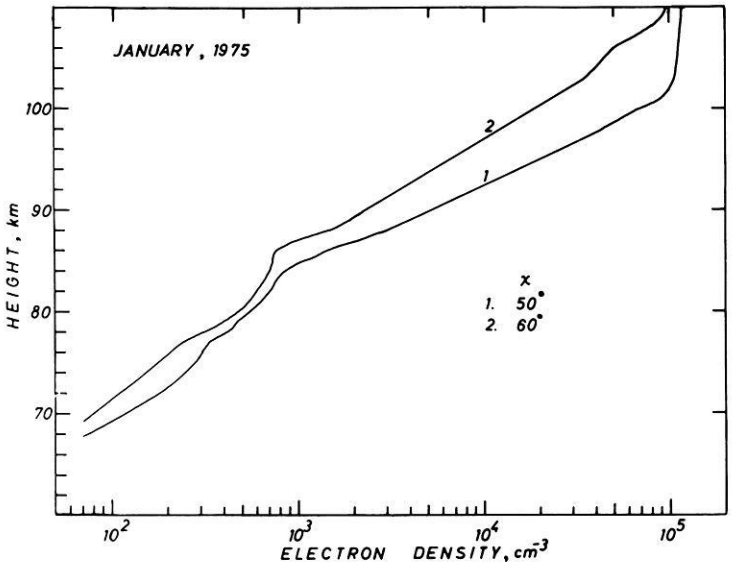

Fig. 4. Same as in Figs. 3, but at SZA 50° and 60° in January, 1975

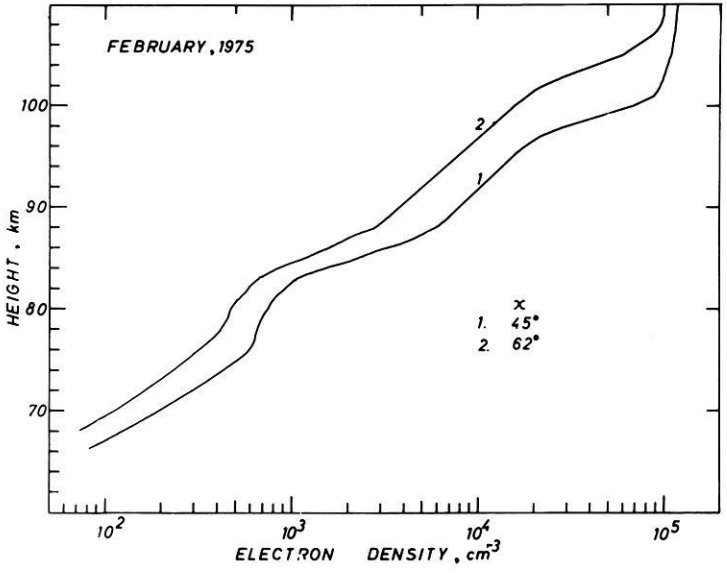

Fig. 5. Same as in Fig. 3, but at SZA 45° and 62° in February, 1975

However, it is found to be lower than α_d at heights above 90 km varying widely to the extent of an order of magnitude with SZA. In contrast, α_{eff} is found to be larger than α_d at heights below 80 km, also varying widely with SZA. Thus it seems that the recombination rates at heights above and below the transition region are not simple or similar processes, such as that of dissociative recom-

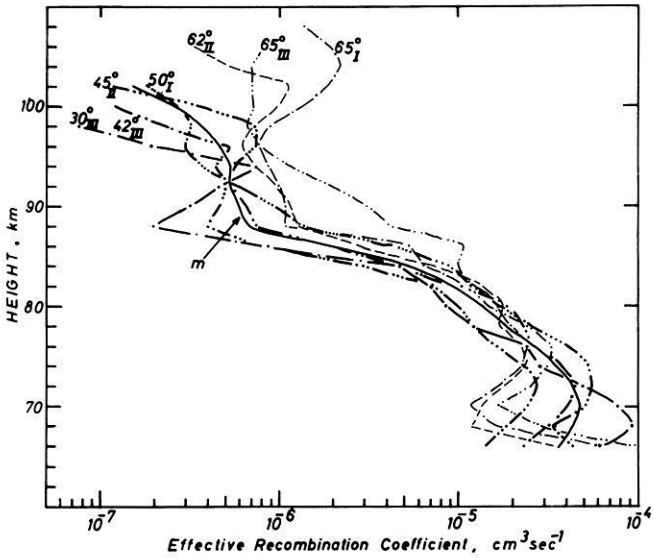

Fig. 6. Effective loss-rate calculated from the profiles of ion production rate and electron density for different solar zenith angles. Suffixes I, II, and III stand for respective months. The *full line curve* marked *m* gives mean α_{eff} for SZA 30°–50°

bination of molecular positive ions. The processes probably involve complex chemistry of cluster ions, negative ions and heavy metallic ions.

8. Conclusions and Discussion

The height-distribution profiles of electron density (N-h) and effective loss-rate ($\alpha_{eff}-h$) are constructed for the height range 65–110 km combining the results of rocket-borne N-h measurements and ground-based partial reflections, A1-absorption and ionosonde measurements for quiet-sun low solar activity conditions at different solar zenith angles in the months of January, February, and March, 1975. It is shown that all the N-h profiles so obtained point to a stratification intermediate between the D-layer maximum and the bottom of the E-layer at about 95 km with Nm around 10^4 electrons/cm^3. Such intermediate maxima had also been observed in some of the rocket flights.

The effective loss-rate is found to be smaller at heights 90–100 km and larger at heights 70–80 km than the dissociative recombination coefficient, varying to the extent of an order of magnitude with change in solar zenith angle and the season.

The low values of α_{eff} at heights above 90 km may be attributed to the presence of some metallic ions which reduce on the average the rate of recombination with electrons. There may be some uncertainty in the radiation fluxes and month-to-month changes in the atmospheric model which may result in low values of ion-production rate and hence give low values of Q/N^2. There is

now sufficient evidence that the ionospheric absorption reduces by about 30% on several occasions when a strong low-type reflecting *Es*-layer occurs at about 95 km (Kotadia et al., 1977). The presence of metallic ions is probably a cause for such strong reflecting sheet of ionization. This fact also supports the intermediate cusp of ionization at 95 km and the low value of α_{eff}. The change in α_{eff} with solar zenith angle also suggests the change in gas composition and hence the relative proportions of various kinds of ions. The high values of α_{eff} at heights below 80 km are probably due to the large influence of negative ions which become almost equal to the number of positive ions at about 70 km during the daytime. These are some explanations for the results reported here, but the chemistry of the lower ionosphere and the ion-kinetics which play important roles in the finer structure of N-h and $\alpha_{eff}-h$ profiles are quite complex and they need to be studied in detail. There is also the case for the investigation of metallic ions in the height range 90–95 km.

Acknowledgements. The authors are very grateful to the scientists of Heinrich Hertz Institute, Academy of Sciences, Berlin (GDR) for their cooperation in establishing a joint research project on ionospheric absorption at Gujarat University, Ahmedabad and for regular discussions and suggestions. One of the authors (A. Gupta) received financial assistance from the Council of Scientific & Industrial Research and the University Grants Commission in the form of research fellowships and contingency grants. We express our due thanks to them also. Very helpful cooperation received from Dr. J.S. Shirke and Dr. S.M. Pradhan of P.R.L. in the construction of N-h profiles with their partial reflection data is gratefully appreciated.

References

Banks, P.: Collision frequencies and energy transfer. Planet. Space Sci. **14**, 1085, 1966

Bremer, J., Singer, W.: Diurnal, seasonal, and solar cycle variations of electron densities in the ionospheric *D*- and *E*-regions. J. Atmos. Terr. Phys. **39**, 25, 1977

Chhipa, G.M., Kotadia, K.M.: Electron density and recombination coefficient profiles obtained in relation to ionospheric absorption and rocket measurements. Ann. Geophys. (Paris)

Cira: COSPAR Working Group IV. Berlin: Akademie Verlag 1972

Groves, G.V.: Atmospheric structure and its variations in the region from 25 to 120 km. Environmental Research Paper No. 368, AFCRL Rep. 71-0410, 1971

Hall, L.A., Schweizer, W., Hinteregger, H.E.: Longterm variation of solar extreme ultraviolet fluxes. J. Geophys. Res. **70**, 2241, 1965

Heraux, L., Higgins, J.E.: Summary of full-disk solar fluxes between 250 and 1940 Å. J. Geophys. Res. **82**, 3307, 1977

Hinteregger, H.E.: The extreme ultraviolet solar spectrum and its variation during a solar cycle. Ann. Geophys. **26**, 547, 1970

Hinteregger, H.E., Hall, L.A., Schmidtke, G.: Solar XUV radiation and neutral particle distribution in July, 1963, thermosphere. Space Res. **5**, 1175, 1965

Horan, D.M.: Coronal electron temperatures associated with solar flares. Publication No. 70-22133. Washington D.C.: Catholic University of America 1970

Huffman, R.E., Paulsen, D.E., Larrabee, J.C., Cairns, R.B.: Decrease in *D*-region $O_2(1\Delta g)$ photoionization rates resulting from CO_2 absorption. J. Geophys. Res. **76**, 1028, 1971

Ivanov-Kholodnyi, G.S., Firsov, V.V.: Short wave solar radiation spectrum at different activity levels. Geomagn. Aeron. **14**, 331, 1974

Jacchia, L.G.: Revised static models of the thermosphere and exosphere with empirical temperature profiles. Cambridge, Mass. USA: Smithsonian Astrophysical Observatory Special Rep. No. 332, 1971

Kotadia, K.M., Chhipa, G.M., Taubenheim, J.: Differences between A1 absorption values measured with sporadic-*E* and normal *E*-layer reflections. Indian J. Radio Space Phys. **6**, 1, 1977

Loidl, A., Schwentek, H.: Mesospheric molecular oxygen density, pressure, and temperature profiles obtained from measurements of solar *H* Lyman-α radiation. J. Geophys. **44**, 107, 1977

Manson, J.E.: Measurements of the Solar Spectrum between 30 and 128 Å. Solar Phys. **27**, 107, 1972

Mechtly, E.A., Bowhill, S.A.: Changes of lower ionosphere electron density with solar activity. J. Atmos. Terr. Phys. **34**, 1899, 1972

Meira, L.G. Jr.: Rocket measurements of upper atmospheric nitric oxide and their consequences to the lower ionosphere. J. Geophys. Res. **76**, 202, 1971

Piggott, W.R., Thrane, E.V.: The electron densities in the *E*- and *D*-regions above Kjeller. J. Atmos. Terr. Phys. **28**, 467, 1966

Schmidtke, G.: EUV indices for solar-terrestrial relations. Philadelphia: XIX Plen. Meeting of COSPAR, 1976

Swider, W. Jr.: Ionization rates due to the attenuation of 1–100 Å non-flare solar X-rays in the terrestrial atmosphere. Rev. Geophys. **7**, 573, 1969

Taubenheim, J., Subrahmanyam, C.V., Klein, G.: Aeronomic results of neutral nitric oxide densities in the lower ionosphere inferred from electron density profiles. Varna: XVIII COSPAR Meeting, 1975

Vidal-Madjar, A., Blamont, J.E., Phissamay, B.: Solar lyman alpha changes and related hydrogen density distribution at the earth's exobase (1969–1970) J. Geophys. Res. **78**, 1115, 1973

Received October 31, 1978; Revised Version February 8, 1979; Accepted February 28, 1979